

Confronting B anomalies with atomic physics

G. D'Ambrosio and A. M. Iyer
INFN-Sezione di Napoli, Via Cintia, 80126 Napoli, Italia

F. Piccinini
INFN, Sezione di Pavia, via A. Bassi 6, 27100 Pavia Italy

A.D. Polosa
Dipartimento di Fisica and INFN, Sapienza Università di Roma, P.le Aldo Moro 2, I-00185 Roma, Italy

We consider a simple implementation of a minimal Z' model in the context of the anomalies in the B decays. With the assumption of the primary contribution being due to the electron, implications from the recent measurements on the weak charge of proton Q_W^p and the Caesium atom Q_W^{Cs} are studied. The conclusion is characterized by different limiting behaviour depending on the chirality of the lepton current. The constraints are then compared with those coming from direct searches. This observation is crucial in determining the exact nature of the solution to the anomaly. The bounds on the simplified models from atomic physics are then compared with those from direct searches. We demonstrate that a minor improvement in the atomic physics measurements can be comparable with the bounds from direct searches with possibly better sensitivities for the heavier masses ($\gtrsim 3.9$ TeV). We finally comment on the collider prospect for observing states beyond the realm of resonant production at LHC.

The observation of flavour non-universality in the semi leptonic decays of the B mesons constitutes one of the strongest hints for beyond standard model (BSM) physics. The measurement of the theoretically clean ratio $R_K = \mathcal{B}(B^+ \rightarrow K^+ \mu^+ \mu^-) / \mathcal{B}(B^+ \rightarrow K^+ e^+ e^-)$ [1]

$$R_K|_{q^2=1-6 \text{ GeV}^2} = 0.745_{-0.074}^{+0.090} (stat) \pm 0.036 (syst)$$

signaled a $\sim 2.6 \sigma$ deviation from the standard model (SM) prediction of $R_K^{SM} = 1.0003 \pm 0.0001$ [2, 3]. Similarly, the measurement of $R_{K^*} = \mathcal{B}(B^0 \rightarrow K^{*0} \mu^+ \mu^-) / \mathcal{B}(B^0 \rightarrow K^{*0} e^+ e^-)$ [4]:

$$R_{K^*} = \begin{cases} 0.660_{-0.070}^{+0.110} (stat) \pm 0.024 (syst), & \text{low } q^2 \\ 0.685_{-0.069}^{+0.113} (stat) \pm 0.047 (syst), & \text{med } q^2 \end{cases} \quad (1)$$

presented a similar picture to that of R_K . A comparison with the SM prediction, leads to a 2.4σ deviation for low q^2 and $\sim 2.5 \sigma$ for medium q^2 . The reported deviations can be parametrized in terms of additional contributions to the Wilson coefficients of the following effective operators:

$$\mathcal{H}_{eff} = -\frac{G_f \alpha}{\sqrt{2}\pi} V_{tb} V_{ts}^* \sum_i \mathcal{O}_{XY} C_{XY} \quad (2)$$

where $C_{XY} = C_{XY}^{SM} + C_{XY}^{NP}$. The observed deviation in the exclusive models for the angular observable P'_5 [5] in $B \rightarrow K^* \mu \mu$ decays by the LHCb [6, 7] and the BELLE [8] experiments suggested the possibility of new physics in the muon sector [9–15]. However, the exclusive modes are characterized by undetermined power corrections making it difficult to separate the NP effects from those of the SM.

There are several fits involving different combinations of Wilson coefficients (WC) for the leptons. [15–19]. In

this letter we will consider the other extreme possibility where the NP couples solely to the electron. One dimensional fits in the basis of Eq. 2 were considered in [19]. In a simplified model with an additional heavy neutral vector, we make the first attempt to study the implications of the explanations of these fits on measurements in atomic physics. Particularly, we are interested in the recent measurements of the weak charge of the proton Q_W^p [20] and the Caesium atom (Q_W^{Cs}). In the SM, it receives contribution due to the following neutral current Lagrangian:

$$\mathcal{L}_{Q_W, Q_F} = \frac{\bar{e} \gamma_\mu \gamma_5 e}{2v^2} \sum_{q=u,d} C_{1q} \bar{q} \gamma^\mu q \quad (3)$$

The tree-level expressions for C_{1q} are given as: $C_{1u} = -\frac{1}{2} + \frac{4}{3} \sin^2_{\theta_W}$, $C_{1d} = \frac{1}{2} - \frac{2}{3} \sin^2_{\theta_W}$

The SM values for C_{1q} are: $C_{1u}^{SM} = -0.1887 \pm 0.0022$ and $C_{1d}^{SM} = 0.3419 \pm 0.0025$. The expressions for the weak charge of the proton and Caesium atom (in terms of C_{1q}) are given as:

$$\begin{aligned} Q_W^p &= -2 [2C_{1u} + C_{1d}] \\ Q_W^{Cs} &= -2 [55(2C_{1u} + C_{1d}) + 78(C_{1u} + 2C_{1d})] \end{aligned} \quad (4)$$

Following the independent measurements for the proton [20] and the Caesium atom [21], the allowed ranges at 1σ are:

$$Q_W^p = 0.0719 \pm 0.0045 ; \quad Q_W^{Cs} = -72.58(29)_{\text{expt}}(32)_{\text{theory}} \quad (5)$$

The simultaneous compatibility of both these measurements is illustrated in Fig. 1. It gives the corresponding 2σ ranges allowed by the measurement of weak charge of proton (gray) and Caesium (brown) in the $C_{1u} - C_{1d}$

plane. The central value in the SM is represented by the black point and lies in the region of overlap due to both experiments. The left plot gives the range for the weak charge measurements of the proton where the theoretical and experimental errors in Eq. 5 are added in quadrature while the right plot corresponds to the linear sum. As expected, with the errors added linearly, the SM exhibits a greater degree of consistency with the measurements. To facilitate comparison with [20], we will restrict our analysis to the errors being added in quadrature. Any NP contribution to either the C_{1u} or C_{1d} must satisfy the constraints from both the measurements simultaneously and will be the focus of the following discussion.

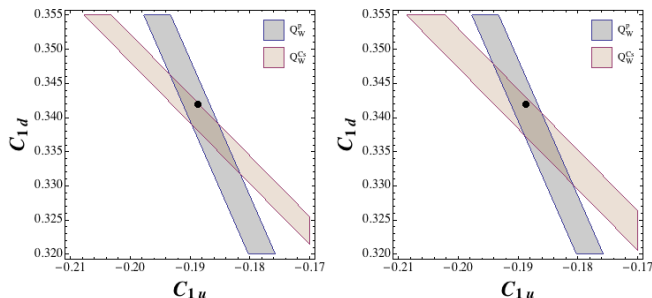


FIG. 1. Allowed regions in the $C_{1u}C_{1d}$ plane due to measurements of weak charge of proton (gray) and Caesium (brown). The central value in the SM is represented by the black point. The left plot corresponds to the error in Eq. 5 added in quadrature while the right corresponds to the linear sum.

New physics contributions

The coefficients C_{1q} in Eq. 3 can receive corrections due to different extensions of the SM. They can be induced either at tree level due to the direct exchange of heavy vectors or at one-loop. Before we discuss a specific implementation of a well defined NP scenario, we consider a generic NP contribution to Eq. 4 as:

$$\mathcal{L}_{NP} = \frac{\bar{e}\gamma_\mu\gamma_5e}{\Lambda^2} \sum_{q=u,d} C_{1q}^{NP} \bar{q}\gamma^\mu q = \frac{\bar{e}\gamma_\mu\gamma_5e}{2v^2} \sum_{q=u,d} C_{1q}^{NP} \bar{q}\gamma^\mu q \quad (6)$$

where we define $C_{1q}^{NP} = \frac{2v^2 C_{1q}^{NP}}{\Lambda^2}$. Note that the appearance of factor $(\frac{1}{v^2})$ in Eq. 6 is to facilitate comparison with the SM contribution in Eq. 3. Combining Eqs. 3 and 6, we get

$$\mathcal{L} = \frac{\bar{e}\gamma_\mu\gamma_5e}{2v^2} \sum_{q=u,d} C_{1q}^{eff} \bar{q}\gamma^\mu q$$

where $C_{1q}^{eff} = C_{1q}^{SM} + C_{1q}^{NP}$ and correspondingly lead to corrections to Eq. 4. Similar to the SM, the C_{1q}^{NP}

(C_{1q}^{NP} to be precise) can be factored into the NP axial vector coupling to electrons (g_e^{AV}) and the vector coupling to light quarks (g_q^V) and can be expressed as: $C_{1q}^{NP} = g_q^V g_e^{AV}$. The range of these couplings can be influenced by observations in other flavour sectors which could be limited by the allowed regions in Fig. 1. Implications of the measurements of Q_W^p and Q_W^{Cs} on NP parameters have been considered in [22–25]. In the following, we consider an effective model with a heavy neutral vector Z' in the context of the observed evidence for lepton flavour universality violation in the semi-leptonic decay of B mesons. Using the observations from atomic physics in different simplified realizations of Z' , we study its impact on the allowed solutions as well as on direct searches.

While the anomalies correspond to a flavour changing observable, $Q_W^{Cs,p}$ is characterized by the flavour diagonal transition. Thus a correlation is possible only with the aid of an underlying model characterized by a flavour symmetry. We fit the Wilson coefficients for the anomalies at B meson scale and determine the correlation between the different couplings. This correlation between the couplings g_q, g_e is then used to compute its effects on the C_{1q} which are determined at $q^2 = 0$. We now discuss a minimal model of heavy neutral vectors which can facilitate this correlation.

Minimal Z' model: Models with additional heavy gauge bosons can be considered a consequence of an extended gauge symmetry *viz.* $U(1), SU(2)$ etc. [26]. Alternatively, these states could also manifest as Kaluza-Klein excitations of gauge fields in extra-dimensional models. [27]. A minimal framework in the context of B anomalies, but with muons, was considered in [28].

The pattern of the FCNC couplings is determined by the structure of the couplings of the fermions to the gauge bosons. Assuming the up-quarks to be in the mass basis, the rotation matrix in the down sector is $D_L = V_{CKM}$. While the left handed rotation is set by charged current couplings, there remains an ambiguity in the form of the right handed rotation matrix. For simplicity we assume the rotation matrix for down type singlets to also follow $D_R \sim V_{CKM}$. The model assumes a $U(2)$ flavour symmetry in the coupling of the quarks to the Z' : irrespective of the chirality we require $g_q = g_s = g_d$ to NP. This is essential in obtaining a V_{CKM} like scaling in order to satisfy the constraints from $\Delta F = 2$ processes [29, 30]. With this background, the most general Lagrangian, after electroweak symmetry breaking, responsible for $b \rightarrow s$

transitions in a Z' model can be parametrized as:

$$\begin{aligned} \mathcal{L} = & \frac{Z'^\mu}{2 \cos \theta_w} [g_e(g'_e)\bar{e}\gamma_\mu P_{L(R)}e + g_\mu(g'_\mu)\bar{\mu}\gamma_\mu P_{L(R)}\mu \\ & + \sum_q (g_q\bar{q}\gamma_\mu P_{LQ} + g'_q\bar{q}\gamma_\mu P_{RQ}) \\ & + (g_t - g_q)V_{ts}^*V_{tb}\bar{s}\gamma_\mu P_{L,R}b + \dots] \end{aligned} \quad (7)$$

Z-Z' mixing: Depending on the underlying framework, the extent of mixing of the SM Z with the Z' can affect the electroweak precision observables. The mixing could be induced by vacuum expectation value (vev), kinetic mixing or loop induced. Since we attempt to represent a wide category of Z' scenarios we assume a mass mixing of the form $c\frac{m_Z^2}{m_{Z'}^2}$ where $c \sim \mathcal{O}(1)$. For simplicity we assume $c = 1$. This gives a contribution to the $Z \rightarrow f\bar{f}$ coupling of the form $g_f\frac{m_Z^2}{m_{Z'}^2}$, where g_f is the Z' - $f\bar{f}$ coupling. The constraint on the size of g_f for the leptons from $Z - Z'$ mixing is particularly strong which translate into an upper bound on g_f as $g_f\frac{m_Z^2}{m_{Z'}^2} \lesssim 0.001$. For cases where $\mathcal{O}(1)$ parameter is 1, leads to a relatively stronger upper bound on g_l . However, one can relax these bounds if the gauge symmetry is extended to a custodial symmetry with the fermions embedded in custodial representations [31–33]. In parallel, this mixing could be also induced at loop level [34] or a kinematic mixing with a small mixing parameter [35] enabling a relaxation of the constraints. In order to represent a significant fraction of Z' scenarios, in this analysis we assume $g_f\frac{m_Z^2}{m_{Z'}^2}$ to be at-most ~ 0.001 .

Anomalies: Independent of the underlying framework the structure of the Wilson coefficient contributing to $b \rightarrow sll$ decays remains similar. There exist several possibilities for the solutions to the anomalies: chirality of the quark and lepton current as well as the lepton identity. Since we are interested in developing a correlation with atomic physics experiments involving electrons, we will only consider the cases where the electron contributions to the NP Wilson coefficients are non-negligible.

Electron only: Since we assume the contribution to the Wilson coefficients due to the muon to be negligible, we set $g_\mu \lll g_e$ in Eq. 7. Fits involving only the electrons were considered in [19] for different combinations of chirality of the quark and the lepton current. The best fit point and the corresponding 2σ ranges for the Wilson coefficients are given in Table I. For each of the fits, it is assumed that only the corresponding Wilson coefficients in the second column of Table I contributes while the others are vanishing. Corresponding to Table I we discuss each of the possibilities below:

Case A $g'_e = 0$: This is the case where the right handed lepton current in Eq. 7 vanishes. Additionally we assume a $U(3)$ symmetry in the coupling of the singlets to the Z' resulting in the absence of tree level FCNC for the

	WC	operator	Best fit	2σ
Case A	C_{LL}	$(\bar{s}_L\gamma^\mu b_L)(\bar{e}_L\gamma_\mu e_L)$	0.99	[0.37,1.61]
Case B	C_{LR}	$(\bar{s}_L\gamma^\mu b_L)(\bar{e}_R\gamma_\mu e_R)$	-3.46	[-4.76,-2.16]
Case C	C_{RR}	$(\bar{s}_R\gamma^\mu b_R)(\bar{e}_R\gamma_\mu e_R)$	-3.63	[-5.5,-2.67]

TABLE I. 2σ ranges used for the fits to Wilson coefficients in the case where only electron couples to New Physics.

down type singlets. Using Eq. 2 and Eq. 7, the Wilson coefficient C_{LL} contributing to $b \rightarrow sll$ processes is given as:

$$C_{LL} = \frac{\sqrt{2}\pi g_e(g_t - g_q)}{4 \cos^2 \theta_W m_Z^2 G_F \alpha} \quad (8)$$

For the first two generations, we assume a $L \leftrightarrow R$ symmetry in the coupling to Z' resulting in $g_V^q = g_q$. For the electron the axial vector coupling is simply $g_e^{AV} = g_e/2$. Using this,, the coefficients C_{1q}^q get corrected as

$$C_{1q}^{eff} = C_{1q}^{SM} + \frac{2v^2 g_e g_q}{8 \cos^2 \theta_W m_Z^2} \quad (9)$$

The additional factor of $\frac{1}{4 \cos^2 \theta_W}$ is due to the form of the Z' Lagrangian in Eq. 7. The following ranges are chosen for the fermion couplings:

$$g_e \in [0.02, 2] \quad g_t \in [0.02, 2] \quad g_q \in [0.02, 2] \quad (10)$$

These ranges are chosen in general and appropriate constraint on the value of g_e is applied for the corresponding mass. The upper bound is chosen such that $g^2/4\pi \leq 1$. The upper bound of ‘2’ is chosen so as to be consistent with an $\sim \mathcal{O}(1)$ parametrisation of couplings. Note that this is well below the rough perturbativity bound $g^2/4\pi$. As we shall see below the results do not depend on the upper limit of the numerical scans. Left plot of Fig. 2 gives the overlap of the region satisfying the anomaly (blue) superimposed on Fig. 1. The black point denotes the SM prediction. The length of the blue band satisfying the anomalies is determined by scanning the allowed ranges for the coupling parameters. Irrespective of the length, Fig. 2 illustrates that there exists only a marginal region common to fit involving Eq. 8 and the anomalies. To represent the change in the ranges of the quark couplings we define:

$$CDF(x) = \int_{-\infty}^x \mathcal{P}(x) dx \quad (11)$$

This can be understood as follows: Let X be a given set of solutions. For a given point on the x axis, the CDF expresses the percentage of solutions in X such that $X \leq x$. $CDF = 1$ at a given x_a implies all solutions satisfy $X \leq x_a$. Top right plot of Fig. 2 gives the CDF for the light quark coupling g_q . The uniform increase in the CDF for the blue curve is indicative of the fact that the range $[0, 1.8]$ is admissible. The red curve on the other hand corresponds to the case when the limits from atomic physics are imposed. It rises rapidly and reaches ~ 1 at

around $g_q \sim 0.23$ which corresponds to the maximum allowed value. Note that the case $g_q \rightarrow 0$ is admitted by both the anomaly solutions as well as the atomic physics. It represents the limiting case $C_{1q}^{eff} \simeq C_{1q}^{SM}$. This bound will have implications for the direct production cross sections and will be discussed later. Note that when $g_q \rightarrow 0$, the SM limit is recovered. This is a consequence of the fact that for the solutions to the anomalies, the Wilson coefficients are proportional to $(g_t - g_q)$ such that $g_t > g_q$.

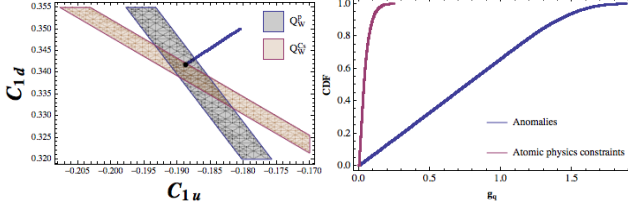


FIG. 2. Results with electron only fits for Case A. Left plot gives the projection on the $C_{1u} - C_{1d}$ plane, while the right plot represents the changes in the range for g_q . The blue (red) curve represents the CDF before (after) the imposition of atomic physics constraints.

Case B $g_e = 0$: This corresponds to the case where the NP contribution to the Wilson coefficients is only due to the right handed electron (C'_{LR}) and the corresponding ranges are given in the second row of Table I. The Wilson coefficient in this case is given as:

$$C'_{LR} = \frac{\sqrt{2}\pi g'_e (g_t - g_q)}{4 \cos^2 \theta_W m_{Z'}^2 G_F \alpha} \quad (12)$$

It is important to note that the sign is reversed relative to Case A. We consider an implementation of the coupling ranges similar to Case A. The negative value is only possible for $g_q > g_t$. Since only the right handed electron current couples to new physics, the corresponding axial vector current is simply $g_e^{AV} = -g'_e/2$. For the light quark case we first begin with the assumption of $L \leftrightarrow R$ symmetry: $g_q = g'_q$. In this case, the coefficients C_{1q} get corrected as

$$C_{1q} = C_{1q}^{SM} - \frac{2v^2 g'_e g_q}{8 \cos^2 \theta_W m_{Z'}^2} \quad (13)$$

The results are illustrated in the top left plot of Fig. 3. Unlike Case A, the limiting case does not reduce to the SM as seen in the top left plot of Fig 3. This is a consequence of the fact that for the solutions to the anomalies, the Wilson coefficients are negative. They are proportional to $(g_t - g_q)$ where $g_q > g_t$. Thus $g_q \rightarrow 0$ is not permitted. However, these solutions are not compatible with the constraints from atomic physics. This is due to the fact that relatively large contributions to C_{1q} are due to g_q and the fact that $g_q^V = g_q$. If we assume $g_q \gg g'_q$

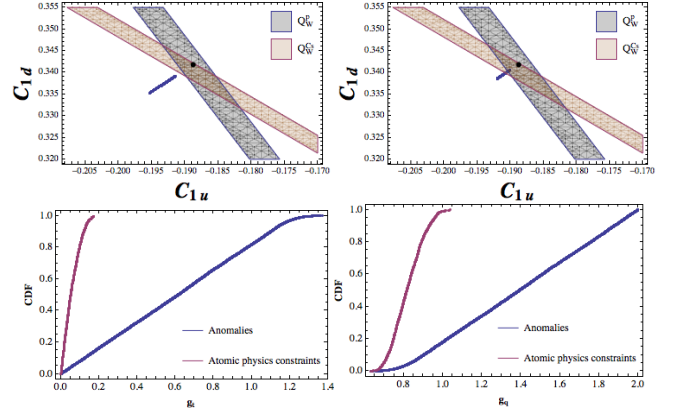


FIG. 3. Results with electron only fits for Case B. Top left plot corresponds to the case $g_q = g'_q$ while the top right corresponds to $g_q \gg g'_q$. The bottom plots gives the changes in the range for g_t (left) and g_q (right) corresponding to the case $g_q \gg g'_q$.

i.e. no $L \rightarrow R$ symmetry, then $g_q^V = g_q/2$ and the coefficients C_{1q} now get corrected as:

$$C_{1q} = C_{1q}^{SM} - \frac{2v^2 g'_e g_q}{16 \cos^2 \theta_W m_{Z'}^2} \quad (14)$$

The corresponding results are now shown in the top right plot of Fig. 3. The agreement with the atomic physics constraints is due to the reduction of the numerical value of g_q^V with respect to the case with $L \leftrightarrow R$ symmetry for the light quarks. Such a framework can be arranged for instance in a warped framework where the doublets are more composite than the singlets, while compromising the explanation of the hierarchy of Yukawa couplings. It has to be noted in this case that the minimum required coupling for the coupling of right handed electron (g'_e) is at the edge of $g'_e \frac{m_{Z'}^2}{m_{Z'}^2} \simeq 0.001$. However, it can be more easily accommodated if, for instance, we assume a minor departure from $\mathcal{O}(1)$ mixing.

Case C $g_e = 0$: This case is similar to B, with the only difference being the presence of FCNC in the singlet sector as opposed to the doublets. Given that the ranges in Table I are similar for B and C, one can expect similar results in terms of the ranges of the couplings for both the cases. The only difference between B and C would be that a consistent set of solutions would necessitate $g'_q \gg g_q$ in this case.

COLLIDER IMPLICATIONS

The solutions consistent with the constraints from atomic physics also have an interplay with direct searches. We discuss this correlation in the context of the cases discussed above:

Case A: In this scenario, the limiting case being the SM ($g_q \rightarrow 0$), strong upper bounds were obtained on the value of g_q and hence the Z' production cross section. It will be interesting to compare it with the bound from direct searches. In a Z' model with coupling to electrons, there exists strong limits from direct searches for both ATLAS [36] and CMS [37]. For instance for a 3 TeV resonance decaying into ee , there is an upper bound on $\sigma \times B.R. < 0.5$ fb. Since the solutions to the anomalies correlate the coupling of the light quarks to those of the third generation as well as leptons, upper bounds on g_q and correspondingly $\sigma_{Z'}$ can be obtained and compared with those obtained from direct searches. In the first instance, we assume 100% branching fraction in the electrons. Consider the case where the coupling to the muons is zero. Left plot of Fig. 4 gives the change in the magnitude of light quark coupling for a 3 TeV resonance with the current (blue) and with 10% improvement in the measurement of Q_W^{Cs} . The corresponding changes in the cross sections are given in the right plot of Fig. 4 for different masses which give the upper bound on $\sigma_{Z'}$ for different benchmark masses. The upper bound on $\sigma \times B(Z' \rightarrow ee)$ for the corresponding masses is given by the solid black line corresponding to the values extracted from [36]¹. The significance of this result lies in the fact that even with an unrealistic assumption of 100% branching fraction into electrons, a mild improvement in the APV sensitivity could be comparable with the bounds from direct searches. If one assumes a SM like branching fraction of 3% into electrons, the current sensitivity is roughly compatible with the direct searches for masses 3 TeV and higher. Improvements by $\sim 10\%$ is illustrated by the dotted pink line thereby resulting in even better sensitivities. The upper-bound on the computed cross-section ($\sigma_{Z'}$) for masses ≥ 3.9 TeV is better than the those obtained from direct searches where the bounds are computed on the variable $\sigma\mathcal{B}(Z' \rightarrow ee)$. Thus in a given model with a known $\mathcal{B}(Z \rightarrow ee)$, the bound from atomic physics can accommodate only smaller values of $\sigma\mathcal{B}$ than those allowed by direct searches. LHC is also sensitive to probing non resonant NP effects by exploring event multiplicity at the tail of the di-lepton p_T spectrum [38]. As an illustration we consider a non-resonant 10 TeV Z' production and explore the event multiplicities in the regime $p_T > 900$ GeV.² Using the CMS card of DELPHES 3 [42], we extract events with two isolated electrons, with the leading electron satisfying $p_T > 900$ GeV. The events are then distributed into bins of size 100 GeV

each and we compute the following variable [43]:

$$Z = \sqrt{\sum_i \left(2(s_i + b_i) \log \left[1 + \frac{s_i}{b_i} \right] - 2s_i \right)} \quad (15)$$

where $s_i(b_i)$ are the signal(background) events in the i^{th} bin. The variable Z is a measure of the signal sensitivity over the background expectation and is sensitive to the differences in events in individual bins. Bottom left plot of Fig. 4 gives the signal discovery significance over the background as a function of the integrated luminosity. It clearly illustrates the sensitivity of the LHC in probing the tail of the p_T distribution. The right plot gives the parameter space of couplings that can be probed at $3 ab^{-1}$. The shaded regions indicate the corresponding signal sensitivity. A correlation between atomic physics and such indirect signatures would be interesting as a future exercise.

Constraints from atomic physics also have implications for the partial decay width of the Z' into fermions. Note that in most models $Z' \rightarrow t\bar{t}$ constitutes the most likely channel for discovery. As shown in the top bottom right plot of Fig. 3, the allowed top-quark coupling to Z' also reduces after the bounds from weak charge measurements. For a 3 TeV resonance, the maximum allowed width is ~ 100 GeV when only the anomalies are taken into account. However, atomic physics measurements reduce the maximum allowed coupling as shown by the red curve, thereby reducing the partial width to ~ 30 GeV. While these constraints increasingly favour a narrow width for the resonance enhancing the chances for discovery, $(\sigma B)_{max}$ could be beyond the sensitivity of the LHC. It is to be noted that the electron coupling does not change drastically before and after the imposition of the atomic physics constraints. After the imposition of the latter, the branching fraction into $t\bar{t}$ becomes comparable to that of ee .

Case B(and C:) This scenario is distinctly different from Case A owing to the opposite sign of the Wilson coefficients as required by the B anomalies. As a result the coupling to the light quarks g_q is always greater than g_t . In this case the features of the branching fraction into a top-quark pair can be classified into the following two categories:

1) $L \leftrightarrow R$ symmetry for the top couplings: With the assumption of $g_L^t = g_R^t$ and with $g_e > g_{L,R}^t$, will result in a comparatively lower branching fraction into a top-quark pair. Thus leptons are likely to constitute the most likely discovery mode.

2) $g_L^t < g_R^t$ for Case B: Since the flavour diagonal coupling of the top singlets is a free parameter, one can also accommodate a larger value of its coupling. This results in the possibility of a larger branching fraction compared to scenario 1. A similar argument also applies to Case C with the difference that the coupling of the top doublets

¹ For a 4 TeV resonance we assume $\sigma B < 1$ fb.

² The model file for the signal is generated using FEYNRULES [39] and matrix element for the process is produced using MADGRAPH [40]. We use PYTHIA 8 [41] for the showering and hadronization.

is a free parameter and one can accommodate $g_L^t > g_R^t$. A large deviation between the coupling of the two chiralities will also result in a forward backward asymmetry. However, updated analysis from TEVATRON [44] would strongly disfavour this scenario.

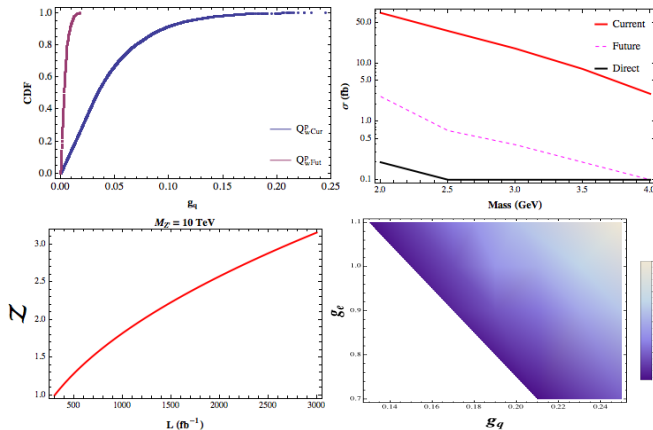


FIG. 4. Top: left plot gives the change in g_q with 10% improvement in Q_W^{Cs} for a 3 TeV mass. Right plot gives the computation of the maximum allowed cross section with current (red) and after (pink dotted) improvement of Q_W^{Cs} . Bottom: The plots illustrate the reach for a 10 TeV resonance. The left gives the signal sensitivity as a function of the integrated luminosity using the current bounds for atomic physics. The right plot gives the corresponding regions in the $g_q - g_e$ space that can be probed at 3 ab^{-1} with shading representing the corresponding sensitivity.

CONCLUSIONS

In a simplified model with a neutral heavy vector Z' , we study the correlation between the (electron only) solutions to the B anomalies and weak charge measurements of proton and Caesium atom. We demonstrate that the extent of consistency with the weak charge measurements is marginal. Depending on the assumption of the chirality of the electron current coupling to Z' , the corresponding limiting behaviour in the $C_{1u} - C_{1d}$ plane is different, thereby serving as a useful discriminant between different patterns of solutions. Irrespective of the form of solutions to the anomalies, weak charge measurements impose bounds on the values of the coupling to Z' . This strongly motivates the need for possible future improvements in Q_W^{Cs} and Q_W^p [45] where the bounds on the couplings especially for the heavier masses can significantly improve those from direct searches.

ACKNOWLEDGMENTS

We are grateful to G. Isidori, F. Mahmoudi and M. Nardecchia for several useful comments and a careful

reading of the manuscript. We are also grateful to F. Feruglio for useful discussions at the beginning of the project. We are grateful to F. Conventi and E. Rossi for discussions on statistical significance. G.D. and A.I. are supported in part by MIUR under Project No. 2015P5SBHT and by the INFN research initiative ENP.

-
- [1] R. Aaij *et al.* (LHCb), Phys. Rev. Lett. **113**, 151601 (2014), arXiv:1406.6482 [hep-ex].
 - [2] C. Bobeth, G. Hiller, and G. Piranishvili, JHEP **12**, 040 (2007), arXiv:0709.4174 [hep-ph].
 - [3] M. Bordone, G. Isidori, and A. Pattori, Eur. Phys. J. **C76**, 440 (2016), arXiv:1605.07633 [hep-ph].
 - [4] R. Aaij *et al.* (LHCb), JHEP **08**, 055 (2017), arXiv:1705.05802 [hep-ex].
 - [5] S. Descotes-Genon, J. Matias, M. Ramon, and J. Virto, JHEP **01**, 048 (2013), arXiv:1207.2753 [hep-ph].
 - [6] R. Aaij *et al.* (LHCb), Phys. Rev. Lett. **111**, 191801 (2013), arXiv:1308.1707 [hep-ex].
 - [7] R. Aaij *et al.* (LHCb), JHEP **02**, 104 (2016), arXiv:1512.04442 [hep-ex].
 - [8] S. Wehle *et al.* (Belle), Phys. Rev. Lett. **118**, 111801 (2017), arXiv:1612.05014 [hep-ex].
 - [9] S. Descotes-Genon, J. Matias, and J. Virto, Phys. Rev. **D88**, 074002 (2013), arXiv:1307.5683 [hep-ph].
 - [10] F. Beaujean, C. Bobeth, and D. van Dyk, Eur. Phys. J. **C74**, 2897 (2014), [Erratum: Eur. Phys. J. **C74**, 3179(2014)], arXiv:1310.2478 [hep-ph].
 - [11] R. Alonso, B. Grinstein, and J. Martin Camalich, Phys. Rev. Lett. **113**, 241802 (2014), arXiv:1407.7044 [hep-ph].
 - [12] T. Hurth and F. Mahmoudi, JHEP **04**, 097 (2014), arXiv:1312.5267 [hep-ph].
 - [13] D. Ghosh, M. Nardecchia, and S. A. Renner, JHEP **12**, 131 (2014), arXiv:1408.4097 [hep-ph].
 - [14] G. Hiller and M. Schmaltz, Phys. Rev. **D90**, 054014 (2014), arXiv:1408.1627 [hep-ph].
 - [15] T. Hurth, F. Mahmoudi, and S. Neshatpour, JHEP **12**, 053 (2014), arXiv:1410.4545 [hep-ph].
 - [16] T. Hurth, F. Mahmoudi, and S. Neshatpour, Nucl. Phys. **B909**, 737 (2016), arXiv:1603.00865 [hep-ph].
 - [17] W. Altmannshofer, P. Stangl, and D. M. Straub, Phys. Rev. **D96**, 055008 (2017), arXiv:1704.05435 [hep-ph].
 - [18] B. Capdevila, A. Crivellin, S. Descotes-Genon, J. Matias, and J. Virto, (2017), arXiv:1704.05340 [hep-ph].
 - [19] G. D'Amico, M. Nardecchia, P. Panci, F. Sannino, A. Strumia, R. Torre, and A. Urbano, JHEP **09**, 010 (2017), arXiv:1704.05438 [hep-ph].
 - [20] D. Androi *et al.* (Qweak), Nature **557**, 207 (2018).
 - [21] V. A. Dzuba, J. C. Berengut, V. V. Flambaum, and B. Roberts, Phys. Rev. Lett. **109**, 203003 (2012), arXiv:1207.5864 [hep-ph].
 - [22] J. Erler, A. Kurylov, and M. J. Ramsey-Musolf, Phys. Rev. **D68**, 016006 (2003), arXiv:hep-ph/0302149 [hep-ph].
 - [23] C. Bouchiat and P. Fayet, Phys. Lett. **B608**, 87 (2005), arXiv:hep-ph/0410260 [hep-ph].
 - [24] A. Falkowski, M. Gonzalez-Alonso, and K. Mimouni, JHEP **08**, 123 (2017), arXiv:1706.03783 [hep-ph].
 - [25] M. Schmaltz and Y.-M. Zhong, (2018), arXiv:1810.10017 [hep-ph].

- [26] A. Donini, F. Feruglio, J. Matias, and F. Zwirner, Nucl. Phys. **B507**, 51 (1997), arXiv:hep-ph/9705450 [hep-ph].
- [27] T. Gherghetta and A. Pomarol, Nucl. Phys. **B586**, 141 (2000), arXiv:hep-ph/0003129 [hep-ph].
- [28] B. Allanach, F. S. Queiroz, A. Strumia, and S. Sun, Phys. Rev. **D93**, 055045 (2016), [Erratum: Phys. Rev. **D95**, no.11, 119902 (2017)], arXiv:1511.07447 [hep-ph].
- [29] G. Isidori, Y. Nir, and G. Perez, Ann. Rev. Nucl. Part. Sci. **60**, 355 (2010), arXiv:1002.0900 [hep-ph].
- [30] S. Gori, in *Proceedings, 2015 European School of High-Energy Physics (ESHEP2015): Bansko, Bulgaria, September 02 - 15, 2015* (2017) pp. 65–90, arXiv:1610.02629 [hep-ph].
- [31] M. Blanke, A. J. Buras, B. Duling, K. Gemmler, and S. Gori, JHEP **03**, 108 (2009), arXiv:0812.3803 [hep-ph].
- [32] M. Blanke, A. J. Buras, B. Duling, S. Gori, and A. Weiler, JHEP **03**, 001 (2009), arXiv:0809.1073 [hep-ph].
- [33] G. D’Ambrosio and A. M. Iyer, Eur. Phys. J. **C78**, 448 (2018), arXiv:1712.08122 [hep-ph].
- [34] R. Gauld, F. Goertz, and U. Haisch, JHEP **01**, 069 (2014), arXiv:1310.1082 [hep-ph].
- [35] H. Davoudiasl, H.-S. Lee, and W. J. Marciano, Phys. Rev. **D85**, 115019 (2012), arXiv:1203.2947 [hep-ph].
- [36] G. Aad *et al.* (ATLAS), Phys. Rev. **D90**, 052005 (2014), arXiv:1405.4123 [hep-ex].
- [37] C. Collaboration (CMS), (2016), CMS-PAS-EXO-16-031.
- [38] A. Greljo and D. Marzocca, Eur. Phys. J. **C77**, 548 (2017), arXiv:1704.09015 [hep-ph].
- [39] A. Alloul, N. D. Christensen, C. Degrande, C. Duhr, and B. Fuks, Comput. Phys. Commun. **185**, 2250 (2014), arXiv:1310.1921 [hep-ph].
- [40] J. Alwall, R. Frederix, S. Frixione, V. Hirschi, F. Maltoni, O. Mattelaer, H. S. Shao, T. Stelzer, P. Torrielli, and M. Zaro, JHEP **07**, 079 (2014), arXiv:1405.0301 [hep-ph].
- [41] T. Sjostrand, S. Mrenna, and P. Z. Skands, Comput. Phys. Commun. **178**, 852 (2008), arXiv:0710.3820 [hep-ph].
- [42] J. de Favereau, C. Delaere, P. Demin, A. Giammanco, V. Lematre, A. Mertens, and M. Selvaggi (DELPHES 3), JHEP **02**, 057 (2014), arXiv:1307.6346 [hep-ex].
- [43] G. Cowan, “Discovery significance with statistical uncertainty in the background estimate,” <https://www.pp.rhul.ac.uk/~cowan/stat/notes/SigCalcNote.pdf>.
- [44] R. Lysk (CDF, D0), in *10th International Workshop on Top Quark Physics (TOP2017) Braga, Portugal, September 17-22, 2017* (2017) arXiv:1711.09686 [hep-ex].
- [45] D. Becker *et al.*, (2018), arXiv:1802.04759 [nucl-ex].